

## Radiative transfer model in the atmosphere and experimental solar data of Yaounde location

E. Guemene Dountio<sup>1,2\*</sup>, D. Njomo<sup>2</sup>, Efa Fouda<sup>1</sup> and A. Simo<sup>1</sup>

<sup>1</sup>*MINRESI/IRGM/LRE, Ministry of Scientific Research and Innovation, Cameroon*

<sup>2</sup>*University of Yaounde I, Faculty of Science, Department of Physics, LATEE, Cameroon*

**Abstract.** In order to produce simulated data on solar irradiation on the earth's surface, we attempted to improve a tridimensional radiative transfer model which takes into account different inhomogeneities of the atmosphere. Those inhomogeneities have been shown to have a significant effect on solar radiation on the earth's surface.

In this paper, the results of the model are compared with experimental solar data and improvements are made on the model to match the data. Two scales were used to compare numerical results with experimental data. A good correlation was found in the daily scale. For the hourly scale, a polynomial correlation was established between numerical data and experimental data.

*Keywords :* radiative transfer – scattering – atmospheric effects – methods : numerical

### 1. Introduction

Solar energy can be directly used in technological applications such as solar heaters, solar dryers and other solar distillers, photovoltaic generators, etc. The calculation of the thermal performances of these apparatuses can be well studied only if the spectral and angular distribution of solar irradiation is well understood. A good knowledge of the characteristics of the solar radiation is necessary to determine the atmospheric phenomena which influenced its propagation, and consequently lead to a better correction of the sensor's response while receiving a signal from a terrestrial or an outer space sender.

---

\*e-mail: eguemene@yahoo.com

Address: P.O. Box 4110 Yaounde Longkak (Cameroon)

Just a few measuring stations of solar irradiation are operational today and they are not well managed, particularly in developing countries where the maintenance of a park of pyranometers on the ground is difficult and expensive, and measurements are rarely carried out at different wavelengths and angles. In this case, data can be obtained through numerical calculations, by solving the radiative transfer equation (RTE) applied to the earth's atmosphere. One of the major factors attenuating the solar radiation is scattering by clouds. The plane parallel models are not accurate enough to handle inhomogeneities in actual clouds (McKee & Cox 1974; Davies 1978). Several studies showed that these inhomogeneities have significant impacts on the transmitted radiation, calculated either for thick and continuous clouds (Cahalan et al. 1994) or for dispersed clouds (Welch & Wielicki 1984; Barker & Davies 1992). Such structures must be studied with a multi-dimensional radiative transfer model, (Stephens 1988; Evans 1993) which breaks up the angular part of radiance into spherical harmonics while the space part is simply discretized by finite differences. In this paper we intend to make a comparison between the results of this model and the experimental data collected on the Cameroonian site of Yaounde (Nganhou et al. 1982; Efa et al. 1983; Simo et al. 1983; 1984; 1985). The first part is devoted to the description of the model. In the second part, we compare the model with the experimental data while the last part deals with the discussion of the results.

## 2. Material

The hourly solar irradiation data considered in this study have been measured at the Yaounde meteorological station (latitude: 3°52 N; longitude: 11°32 E; altitude: 753 m), using Epley pyranometers associated with Licor integrators (Nganhou et al. 1982). Computations and analysis are done using the Excel 2003 software, while Fortran 90 is the programming tool used for the numerical calculation codes.

## 3. Method

### 3.1 Modelling equation

The Radiative Transfer Equation (RTE) describes in mathematical form, energy exchanges when radiation with a given wavelength  $\lambda$  is propagated according to the  $\Omega$  direction through a volume element. This equation can be written as

$$\begin{aligned} \frac{d}{ds}R_{\lambda}(s, \Omega) &= -[K_{abs}(\lambda, s) + K_{Diff}(\lambda, s)]R_{\lambda}(s, \Omega) + K_{abs}(\lambda, s)L_{0\lambda}[T(s)] \\ &+ \frac{K_{Diff}(\lambda, s)}{4\pi} \int_{4\pi} P(\lambda, s, \Omega', \Omega)R_{\lambda}(s, \Omega')d\Omega' \end{aligned} \quad (1)$$

where:

- $K_{abs}(\lambda, s)$  is the monochromatic absorption coefficient of the particles present in the media and located at  $s$  position; according to the Kirshof law, it is also the emission coefficient of the same particles.
- $K_{Diff}(\lambda, s)$  is the monochromatic scattering coefficient of the particles located at the  $s$  position;
- $L_{0\lambda}[T(s)]$  represents the emission of the black body at temperature  $T$  of the particles located at  $s$ . The presence of the emission term is justified by the fact that any particle at a given temperature radiates. In the present study, considering the spectral range used for measurements, the temperature order of equatorial regions and the accuracy level of sensors, the overall contribution of the emission can be significant. This emission is assumed to be isotropic and as such, simplify calculations by the constancy of the term in all directions.
- $P(\lambda, s, \Omega', \Omega)$  is related to the scattering phase function. It represents the probability that the volume element located in  $s$  has to scatter in direction  $\Omega$ ; radiation which has been propagating originally in  $\Omega'$  direction.
- The term  $\frac{K_{Diff}(\lambda, s)}{4\pi} \int_{4\pi} P(\lambda, s, \Omega', \Omega) R_{\lambda}(s, \Omega') d\Omega'$  called “scattering integral”, represents the total increase of radiation in the considered direction due to the scattering phenomena.

Due to the fact that the medium is discretized spatially according to  $x$ ,  $y$ , and  $z$  directions, the space differential term of equation (1) can be written as follows:

$$\frac{d}{ds} R_{\lambda}(s, \Omega) = \overrightarrow{\nabla R_{\lambda}} \bullet \vec{s} = \cos(\theta) \frac{\partial}{\partial z} R_{\lambda} + \sin(\theta) \cos(\varphi) \frac{\partial}{\partial x} R_{\lambda} + \sin(\theta) \sin(\varphi) \frac{\partial}{\partial y} R_{\lambda} \quad (2)$$

$\theta$  and  $\varphi$  represent the orientation angles of the considered propagating direction.

Media properties are input given a standard tropical atmosphere, with a horizontally uniform distribution of aerosols having a lognormal size distribution. The clouds are essentially made up of liquid water droplets with a gamma distribution of effective particle radii. The cloud particles are assumed to have a Henyey – Greenstein phase function, with asymmetry parameter of 0.85 (Evans 1998). For big size aerosol particles, the absorption coefficient, scattering coefficient and phase function are evaluated using Lorenz-Mie theory, in a correlated k-distribution approach (Fu & Liou 1992). For molecular gases and small size aerosols particles, Rayleigh theory is used and molecular Rayleigh phase function is assumed, in the same correlated k-distribution approach.

Breaking equation (1) into its components, we realize that the model assumes variation of radiance in the media as a result of four atmospheric phenomena. See Fig. 1.

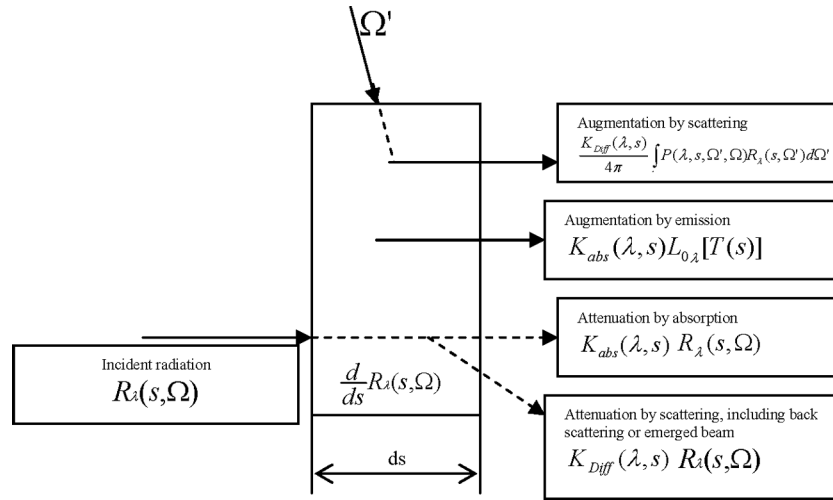


**Figure 1.** Schematic representation of the different components of the radiative transfer equation.

### 3.2 Introduction of spherical harmonics

Any Radiative Transfer Equation (RTE) solving method has its particularities in terms of approximation level (Baudoux 2002). The spherical harmonics method replaces the squaring diagram of the Discrete Ordinate Method (DOM) by a representation of the radiance field in a series of spherical harmonics. The components of the radiance field can thus be evaluated simultaneously according to all directions of space. The accuracy of the results depends however on the truncation of the spherical harmonics base.

$\{y_l^m(\Omega)\}_{|m|\leq l}^{l\leq L}$  indicates the truncated base of the spherical harmonics with the order L. This shows that the scattering integral is reduced to the form of equation (3) (Ou & Liou 1982):

$$\frac{K_{Diff}}{4\pi} \int_{4\pi} P(\Omega', \Omega) R(s, \Omega') d\Omega' \approx K_{Diff} \sum_{l=0}^L \frac{\chi_l}{2l+1} \sum_{m=-l}^l R_l^m(s) Y_l^m(\Omega) \quad (3)$$

where  $R_l^m(s)$  is the order component ( $l, m$ ) of radiance in the spherical harmonics base, as defined by relation (4).

$$R(s, \Omega) \approx \sum_{l=0}^L \sum_{m=-l}^l R_l^m(s) Y_l^m(\Omega) \quad (4)$$

$\chi_l$  is the coefficient of the developed phase function in Legendre polynomials series, defined

by relation (5)

$$P(\cos \theta) \approx \sum_{l=0}^L \chi_l P_l(\cos \theta) \quad (5)$$

Equation (1) becomes

$$\begin{aligned} \cos(\theta) \frac{\partial}{\partial z} R_l^m + \sin(\theta) \cos(\varphi) \frac{\partial}{\partial x} R_l^m + \sin(\theta) \sin(\varphi) \frac{\partial}{\partial y} R_l^m = -(k_{abs} + k_{dif}) R_l^m \\ + k_{abs} L_{0\lambda}^{lm} + k_{dif} \sum_{l=0}^L \frac{\chi_l}{2l+1} \sum_{m=-l}^l R_l^m Y_l^m. \end{aligned} \quad (6)$$

The SHDOM code is thus structured as follows:

1. The RTE is integrated spatially according to each discrete ordinate without taking into account the scattering integral that allows for the initialization of the system.
2. The scattering integral is evaluated using the radiance field calculated at the preceding stage.
3. The RTE is integrated spatially following all the discrete ordinates, taking into account the scattering integral calculated at the preceding stage.
4. Stages 2 and 3 are continued until the results converge following a preset criterion of accuracy.

Looking at the above principles, it can be stated that the Spherical Harmonics Discrete Ordinate Method SHDOM, is an iterative RTE solving method which cumulates the speed of evaluation of the scattering integral on a basis of spherical harmonics with the effectiveness of the calculation of radiation propagation along discrete ordinates in three dimensions of space. The interpolation of the optical properties makes it possible to calculate radiance at any point of the media by taking into account the absorbent and scattering character of the media. Through integration in all directions of space and over a period of time, irradiation is obtained. The method successfully goes through validation tests on 1D, 2D and 3D simulated media (Evans 1998). Its success is all the more significant because it requires less computing time.

### 3.3 Application to solar irradiation calculation

SHDOM was applied to evaluate solar irradiation on the Cameroonian location of Yaounde. Indeed, an outer loop was established taking SHDOM as one of its components. This made it possible for us to calculate hourly irradiation received on the ground, taking into account the geographical positioning parameters of the considered location. The resulting algorithm is presented in Fig. 2.

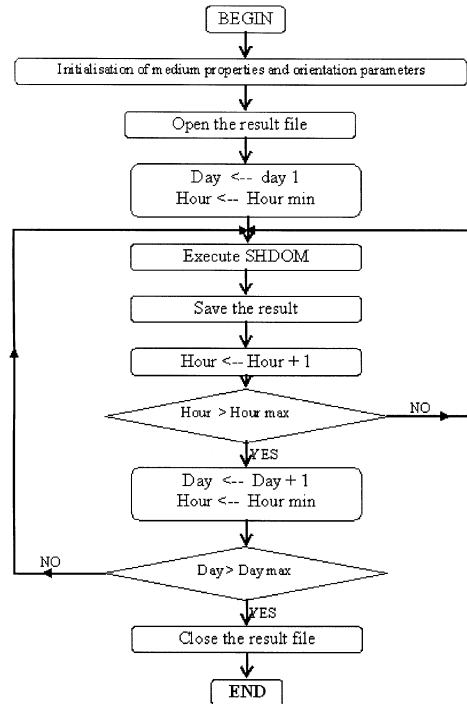


**Figure 2.** Model describing algorithm.

## 4. Results and discussion

The results were obtained after running the code. Since they consist of normal plane radiation (received on a plane perpendicular to the direction of the sun), they were converted to match the results of the experiments by finding their component on horizontal plane and by integrating them in all directions of space. This process enabled us to find the global irradiation on horizontal plane, following a data derived linear correlation, justified by the spectral sensitivity of the sensors and spectral range considered while running the code. Two particular scales were then considered, the hourly scale and the daily one.

### 4.1 Hourly scale

Fig. 3 shows a good agreement with the variation range of solar irradiation, but a poor agreement from one day to another. We assume that it is a consequence of the static character of media properties.

For a better comparison between the model results and experimental data, Fig. 4 has

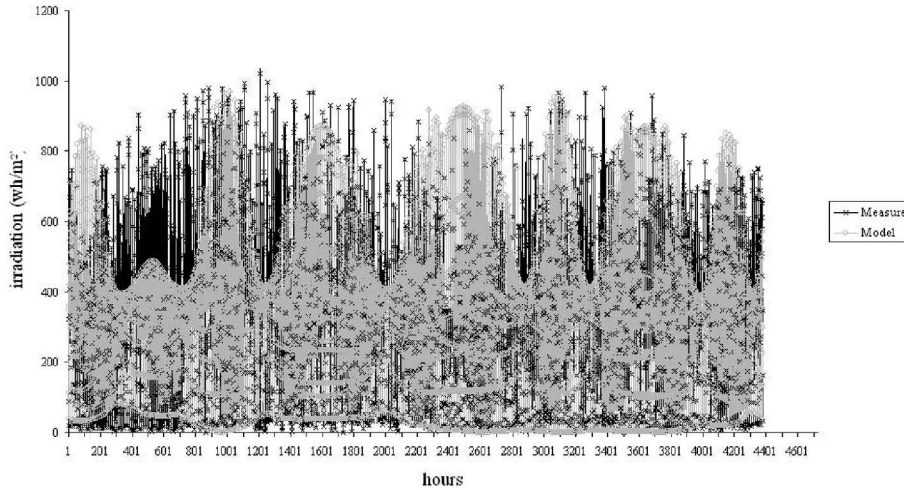


**Figure 3.** Model results and hourly measurements.

been plotted. If the model results were absolutely identical to the experimental data, all the points could have been on the straight line marked as (2) on Fig. 4. But the reality is much more different, and there are a number of sparse points. The sparse points can be linked to overcasts days, which were found by a previous study to constitute more than 18% of the days in Yaounde. Fig. 4 also shows the existence of a polynomial correlation between the model results and measures. The polynomial correlation was found using the least square method, after defining inclusion criterions, to avoid loss of precision induced by sparse points. These criterions are specified by equation (7).

$$\begin{cases} \text{Model} < 600 \\ \text{Model} < \frac{1}{3}\text{Measures} + 400 \end{cases} \quad (7)$$

That results in the regression equation (8).

$$\text{Mesures} \approx a(\text{Model})^2 + b(\text{Model}) + c \quad (8)$$

where  $a = +0.00103$   $b = +0.689$   $c = +3.007$ .

Without any more detailed information on the media properties, this correlation could be used to correct the model results to match the experimental data of Yaounde. In Fig. 4, the correlation is represented by the curve (3).

#### 4.2 Daily scale

Looking at the results shown in Fig. 5, we can make the following remarks:

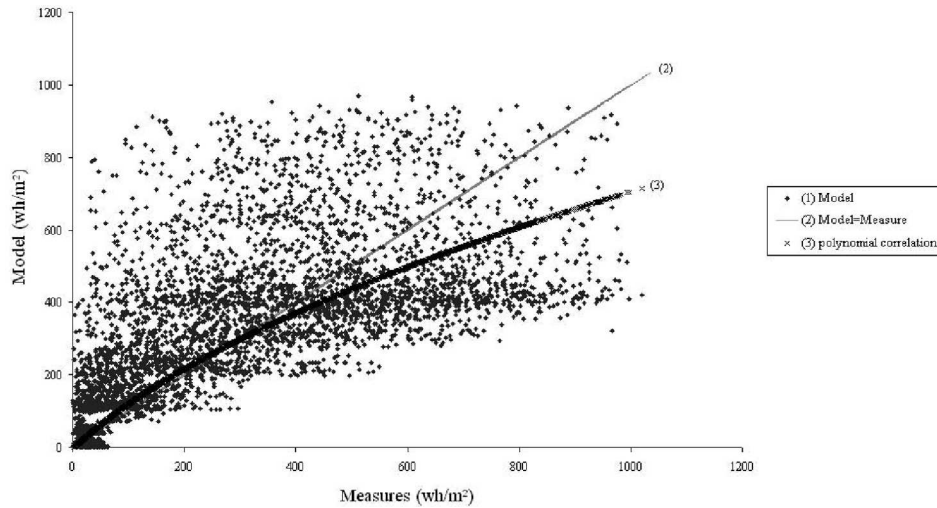


**Figure 4.** Comparison between model results and hourly measurements.

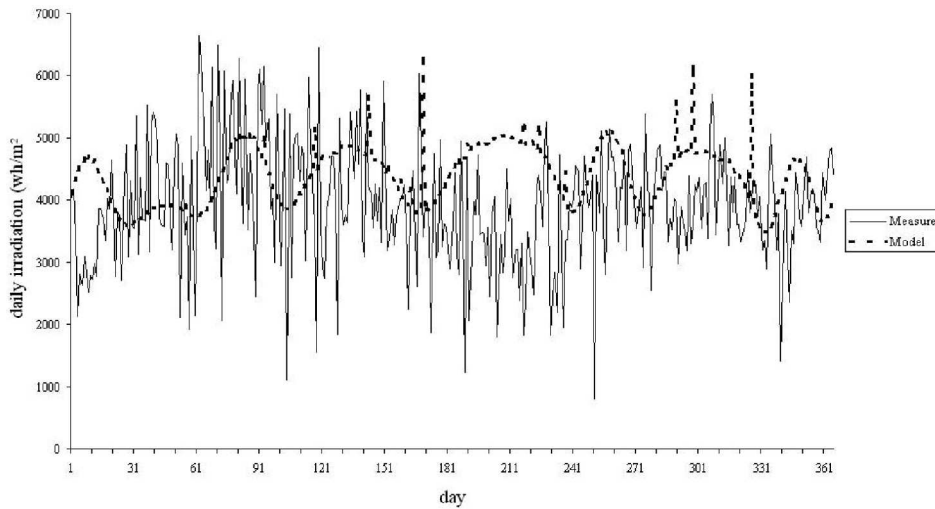


**Figure 5.** Comparison between model results and daily measurements.

In the daily scale, the model presents better results with a good variation range. However, there are differences between measures and results, which may be due to a weak spatial and temporal characterization of the media properties. More information can be obtained after a statistical study of satellite images.

As shown in Table 1, another comparison between the model results and the ex-

**Table 1.** Comparison of model results and experimental data at the daily scale.

	Measures (wh/m <sup>2</sup> )	Model (wh/m <sup>2</sup> )	Ratio Measures/Model
Average	3928	4384	0.9
Standard deviation	982	488	0.2

perimental daily data was done using two statistical parameters, the mean value and the standard deviation, which were calculated in the experimental data population, the model data population and also in a population derived from the two preceding ones, constituted by the ratio of measurements over the model data. This table shows a statistically good agreement between these two populations.

## 5. Conclusion and perspectives

This study reveals a possible correlation between model results and measures according to the hourly scale, and a good agreement between model results and measures according to the daily scale. It also highlights the strengths and weaknesses of the model, particularly its speed and the need for a better characterization of the media. In fact, the differences noted between the experimental data and model data were assumed to be a consequence of a weak characterization of media properties. However, this study confirms the possibility of having acceptable simulated data of the Yaounde location. Equally, this result can considerably reduce the cost of acquisition systems and it can also be directly used for solar systems calibration. With further improvements, the code can be reversed to determine different components of the atmosphere and study their variability.

However, for better results, we believe that further improvements of the model can be done in the light of finding the real reasons for the differences between simulation and measurement, using satellite observations to make a better characterization of the media, including a dynamic consultation of media properties as well as investigating the interaction of solar rays with electrically charged media in order to specify the amount of solar rays whose magnitude is disturbed by the ionosphere layers.

## References

- Barker, H., & Davies, J., 1992, *JAtS*, 49, 1115  
 Baudoux, P., E., 2002, PhD Thesis, Université de Rouen, France  
 Cahalan, R., et al., 1994, *JAtS*, 51, 2434  
 Davies, R., 1978, *JAtS*, 35, 1712  
 Efa Fouda, et al., 1983, *Mes. Ray. Sol. Cam DGRST/IRGM/LRE*, 2, 4  
 Evans, K., F., 1993, *JAtS*, 50, 3111  
 Evans, K., F., 1998, *JAtS*, 55 No. 3, 429  
 Fu, Q., & Liou, K., N., 1992, *JAtS*, 49, 2139

- Mckee, T., & Cox, S., 1974, *JAtS*, 31, 1885  
Nganhou, J., et al. , 1982, *Mes. Ray. Sol. Cam DGRST/IRGM/LRE* , 1, 8  
Ou, S.,C.,S., & Liou, K.,N., 1982, *J.Q.S.R.T.*, 28 No. 4, 271  
Simo, A., Siyam S., S., & Bisseck H., 1983, *Mes. Ray. Sol. Cam DGRST/IRGM/LRE* , 3, 82  
Simo, A., Siyam S., S., & Bisseck H., 1984, *Mes. Ray. Sol. Cam DGRST/IRGM/LRE* , 4, 86  
Simo, A., Siyam S., S., & Bisseck H., 1984, *Mes. Ray. Sol. Cam DGRST/IRGM/LRE* , 5, 90  
Simo, A., Takoudjou, C., & Bisseck H., 1985, *Mes. Ray. Sol. Cam DGRST/IRGM/LRE* , 6, 85  
Stephens, G., 1988, *JAtS*, 45, 1818  
Welch, R., & Wielicki, B., 1984, *JAtS*, 41, 3086